JOURNAL OF Materials CHEMISTRY

Preparation of ordered mesoporous ceria with enhanced thermal stability

Daniel M. Lyons, Kevin M. Ryan and Michael A. Morris*

Materials Section, Department of Chemistry, University College, Cork, Republic of Ireland. E-mail: m.morris@ucc.ie; Fax: +353 21 4274097; Tel: +353 21 4902180

Received 30th May 2001, Accepted 18th December 2001
First published as an Advance Article on the web 12th February 2002

The use of neutral surfactants to form a thermally stable ordered mesoporous ceria phase is reported. The judicious choice of cerium acetate as the inorganic framework precursor and the inorganic to surfactant ratio in the preparation mixture allowed the condensation of acetate derived inorganic polymer chains about the surfactant phase to form a regular mesoscopically ordered inorganic–organic matrix. Even at the low temperature processing conditions used to prepare the hybrid matrix the cerium precursor was seen to form the fluorite type structure of CeO_2. Careful thermal processing of the matrix allowed the subsequent densification (of the pore walls) of the inorganic component and removal of the organic component so that a high quality ordered and truly crystalline mesoporous ceria was formed. The calcination procedure used resulted in a reduction of the long-range order of the pore channels (as evidenced by powder X-ray diffraction) whilst maintaining directionally aligned mesoporous channels as observed by transmission electron microscopy. These ordered pore structures remained even after high temperature ageing. The templating route adopted was found to allow the facile low temperature removal of surfactant due to the hydrogen bonding nature of the surfactant–ceria interaction. Differential scanning calorimetery (DSC) data are consistent with some amount of rapid ceria lattice reduction (Ce^{4+} to Ce^{3+}) at the surface related to the presence of intimate organic–inorganic interactions most likely the result of hydrogen bonds that exist between the surfactant and the ceria lattice. Any reduction of the ceria pore wall surface during the initial thermal processing is rapidly re-oxidised by rapid mass transport of gas phase oxygen molecules through the open pore system during the process of template removal. The material maintained high surface areas after calcination up to temperatures of 873 K. The preparation of high surface area ceria with a stable uniform array of pores is significant and may allow the development of novel catalytic applications for ceria.

Introduction

Ceria is now the focus of constant and varied research due to its industrial applications in areas such as high temperature ceramics, catalysis and solid oxide fuel cell applications.[1] This is because of its oxygen storage capacity which is based on a unique ability to undergo reversible redox transitions to form a series of non-stoichiometric phases of composition $CeO_2 \rightarrow CeO_{2-x}$ and this underpins the current interest.[2] As a vital component in the so-called three-way catalysts (TWC) for automotive exhaust emission control, ceria has proven useful in several ways; it aids the stabilisation of the alumina washcoat, prevents the inward diffusion of noble metals such as rhodium into the washcoat and prevents those metals being deactivated by being held in high oxidation states.[3] However, it is its oxygen storage capacity (OSC) that gives ceria-based catalysts the unique ability to oxidise unburnt hydrocarbons or reduce nitrous oxides under fuel rich and lean conditions respectively.[4] In many cases, ceria's effectiveness as a catalyst is reduced at elevated temperatures due to sintering and loss of surface area. Much effort has gone into improving the catalytic properties of ceria by enhancing its textural and morphological characteristics or by judicious doping with transition metals or lanthanide oxides to enhance its oxygen storage buffering ability.[5] High surface area ceria has been prepared by a number of methods *viz*. homogeneous precipitation and microemulsion methods.[6] Such compounds by virtue of their large surface area exhibit greater catalytic activity.

With the preparation in 1991 of mesoporous silica by Mobil Oil scientists a new area of chemistry, allowing the exploitation of high surface area materials, was opened up.[7] The use of surfactants as liquid crystal templating agents so as to create a regular three-dimensional micellar array about which an inorganic precursor could form a framework gives a reliable method to produce ordered mesoporous solids. These have become known as MCM's (Mobil Composition of Matter) or MMS's (Mesoporous Molecular Sieves). The subsequent removal of surfactant in a controlled manner yields a material with an open framework with uniform pore dimensions in the range 2–10 nm. This silica-based synthesis has been extended to a number of transition metal and main group oxides using various surfactants and inorganic precursors under different reaction conditions.[8,9] The preparation of disordered mesoporous ceria (such that there is a distribution of pore directions and sizes) by a liquid crystal templating method has been reported.[10] The as-synthesised ceria-template composite had a non-ordered mesoporous structure, as did the material after calcination. The solid did retain relatively high surface areas following the calcination procedure used. Herein is reported a neutral templating method employed to form not only a perfectly ordered ceria-template as-synthesised material but also a true mesoporous ceria of uniform pore direction and size with enhanced stability after surfactant removal.

Experimental

6 g Hexadecylamine as a surfactant was added to 35 ml of a 50% aqueous ethanol solution. This preparation is essentially similar to that of Pinnavaia *et al.*[11] except that in the work

described here a much lower than usual (*e.g.* in the work of Pinnavaia[11] a value of around four for the inorganic precursor : surfactant molar ratio was used) inorganic precursor : surfactant molar ratio of 2 was achieved by adding the required quantity of cerium precursor, in this case as the hydrated acetate ($Ce(C_2H_3O_2)_3 \cdot 1.5H_2O$, 99.99% Alfa Aesar). The mixture was stirred for 1 hour at 298 K and placed in an oven at 333 K for 2 days (ambient atmospheric conditions). The precipitate formed was washed with ethanol–water mixtures and harvested by filtration. The products were again washed with deionised water and were dried in air at 423 K for 6 hours (subsequently described as the as-synthesised material) and then calcined at temperatures from 573 K to 873 K in air for 4 hours. The bulk structural chemistry of all the samples was analysed by powder X-ray diffraction (PXRD) and transmission electron microscopy (TEM). PXRD data were collected on a Philips PW 3710 MPD instrument using Cu-Kα radiation of wavelength $\lambda = 0.154157$ nm in the range 1–5° 2θ and 10–80° 2θ for bulk analysis. An accelerating voltage of 40 kV and current of 30 mA were used. Angle calibration was made by reference to the straight through beam and the reflections from a powdered silicon single crystal. The PXRD data were characterised using Rietveld software analysis. This degree of analysis was required because of the very complex shape relationship of individual reflections. Differential scanning calorimetry in addition to Fourier transform infrared spectroscopy (Perkin Elmer Paragon 1000) was used as a technique for monitoring both the removal of surfactant and bulk phase changes within the composite. Data for the samples were obtained on a Setaram DSC 92 and a CS 92 Controller. TEM images of the mesoporous matrices were collected on a JEOL 1200EX TEMSCAN instrument at an accelerating voltage of 120 kV. For TEM, samples were dispersed ultrasonically in a water–ethanol solution and a drop was placed on a 400 mesh gold grid, and the solvents allowed to evaporate. Surface areas and adsorption isotherms were measured using the multipoint BET method and data was collected on a Micromeritics Gemini 2375 instrument. Samples were outgassed at 473 K for 6 hours prior to analysis.

Results and discussion

Low angle powder X-ray diffraction patterns for uncalcined (as-synthesised) and calcined ceria are shown in Fig. 1. Unlike previously reported[12,13] PXRD patterns, the as-synthesised material shows intense well-defined peaks between 1–5° 2θ. These peaks are assigned in Fig. 1(a) to (100) and a pore-to-pore distance of about 70 Å, (110) and (200) reflections from a pseudo-hexagonal ordering of pores. A repeat distance of about 40 Å is obtained from the PXRD profile after calcination. The term pseudo-hexagonal is used because the positions of the features vary slightly (about 10%) from theoretical calculations for a perfect hexagonal array based on the position of the (100) peak. Very careful angular calibration of the diffractometer (see above) was used to ensure that these effects were not due to instrumental problems such as zero angle misalignment. Further, Rietveld refining of the cubic structure of the silicon powder used for alignment showed that the zero angle was within 0.01° of the ideal. For these reasons, it is suggested that the non-agreement with the expected theoretical positions might be due to various reasons including the pores not being ideally hexagonally stacked (due to regular strains being developed within the structure) or even the formation of ordered but complex hexagonal structures (due possibly to irregularly shaped pores). This latter suggestion might be more likely since it is shown below that the pore walls have well-defined morphologies which might lead to non-regular pore shapes.

Surprisingly, in view of the highly ordered diffraction profiles obtained, TEM micrographs of the uncalcined material do not show any system of well-ordered pores despite considerable efforts at the microscope. It is suggested that this apparent anomaly is probably related to the presence of excess surfactant that prevents clear imaging (Fig. 2(a)). However, calcined

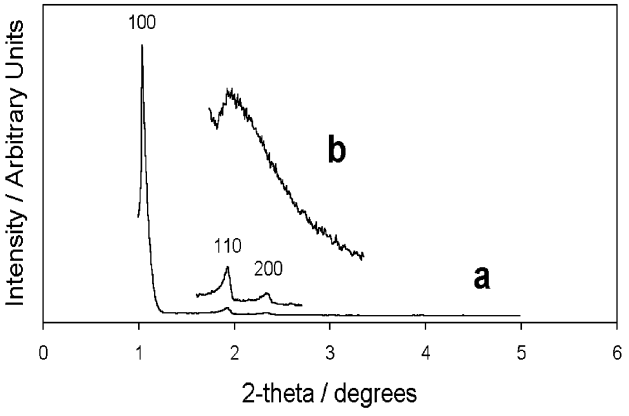

Fig. 1 Low angle PXRD diffractograms of mesoporous ceria (a) uncalcined and (b) calcined in air at 873 K with the corresponding plane assignments. Expanded area is from the diffractogram of uncalcined ceria.

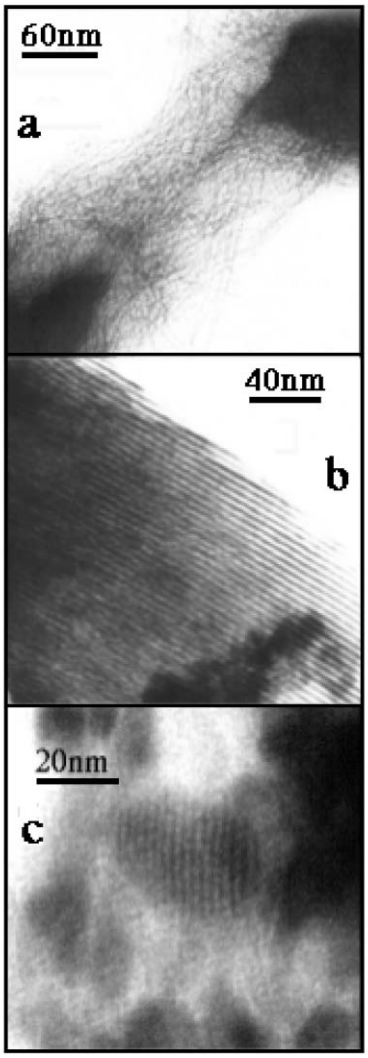

Fig. 2 TEM micrographs of (a) uncalcined ceria–surfactant composite, (b) mesoporous ceria after calcination at 673 K in air and (c) mesoporous ceria calcined in air at 873 K.

materials show many areas of sample to have mesoscopic ordering. Fig. 2(b) shows TEM data for a sample calcined at 673 K which is effective in removing all of the surfactant. The image of an ordered mesoporous ceria product is clearly shown in the figure. PXRD patterns taken for samples calcined at 673 K and 873 K do not display the very highly ordered diffractograms of the as-synthesised material. Instead a single broad feature is seen at about 2° 2θ as shown in Fig. 1(b). At 873 K, despite the poorly defined PXRD profiles, the samples retain highly ordered phases as evidenced by TEM (Fig. 2(c)).

Some comment should be made on the juxtaposition of the TEM and PXRD data. The data can be rationalised in a simple manner; that the calcined materials are essentially non porous and that the TEM images observed result from small residual amounts of mesoporous material. This explanation is rejected on several grounds. Firstly, the area below the mesoporous related diffraction peaks in the PXRD patterns are similar before and after calcinations to 873 K and only decrease by factors above 2 on calcining at temperatures of 973 K and above where all indications of mesoporosity are lost. Further, the high surface areas obtained (see below) and the BET isotherms for the calcined material obtained, which show shapes fully consistent with highly mesoporous materials (typical data are shown in Fig. 3) are also not consistent with this argument. Thus, it is suggested that the calcined material does have aligned pores of uniform size, as seen quite clearly in the TEM micrograph at 873 K. However, on close inspection it can be seen that the pores do not run exactly parallel over their entire length and it is proposed that this lack of directional uniformity probably results in non-coherent scattering and subsequent broadening of all PXRD features such that only the most intense feature (100) can be observed.

As described above, surface areas were in the range expected for such materials. At 573 K a BET surface area of 245 m^2 g^{-1} was obtained, while at 873 K this was reduced to 105 m^2 g^{-1}. This was still significant compared to a surface area of 80 m^2 g^{-1} for a conventionally prepared ceria reference sample after calcination at a temperature of 873 K.[12] It is thus clear from the data obtained here that the synthesis route employed produces an ordered hexagonal mesoporous phase. A similar phase has been reported for reduced ceria produced by complex hydrogen reduction treatment[13] but to the best of our knowledge no such material has been synthesised in ambient conditions for normal unreduced CeO_2 after template removal.

In comparison to data presented by Trovarelli *et al.*[12,13] where cerium chloride was used as the ceria source, the low angle PXRD data shown in our text is of very high quality. It is thought that this is due largely to the use of cerium acetate (rather than the chloride salt) as the ceria source which is more favourable for ordering of the inorganic–organic composite prior to condensation. This is rationalised since acetates have the propensity to form long chain polymeric-type assemblies in solution.[14] This allied with hydrogen bonding between the inorganic and surfactant headgroup provides a useful aid to directing framework organisation about the template. In the work of Trovarelli *et al.* it is stated that cationic template (cetyltrimethylammonium bromide) removal was complete at 923 K.[12] The formation of porous structures may not be possible because of the high calcination temperatures required (even if the authors had shown high quality as-synthesised materials).

A clear advantage of the work reported herein is that IR and DSC measurements confirm that complete removal of hexadecylamine surfactant is achieved at relatively low calcination temperatures of 573 K (see Fig. 4, Fig. 5 and text below) indicating a weaker interaction between the ceria precursor and the template than that observed for a cationic template[12] and this consequently affects the quality of calcined as well as the as-synthesised material. DSC and IR scans for the as-prepared (*i.e.* uncalcined) mesoporous ceria in ambient conditions are described in Fig. 4 and Fig. 5 respectively. In Fig. 5 the IR spectrum recorded for the as-synthesised material shows large broad features assigned to hydrocarbon-related features. On calcination to 573 K there is a dramatic decrease in the intensity of these features so that only water adsorption or related absorption (-OH features at 3400 cm^{-1}) and carbonate (adsorbed bidentate carbonate signals at 1500 and 1280 cm^{-1}) features are observed. The large and well-resolved exotherm in Fig. 4 is obviously associated with oxidation of surfactant within the pore structure. The very sharp, single peak structure of the exotherm contrasts with the complex thermogravimetric

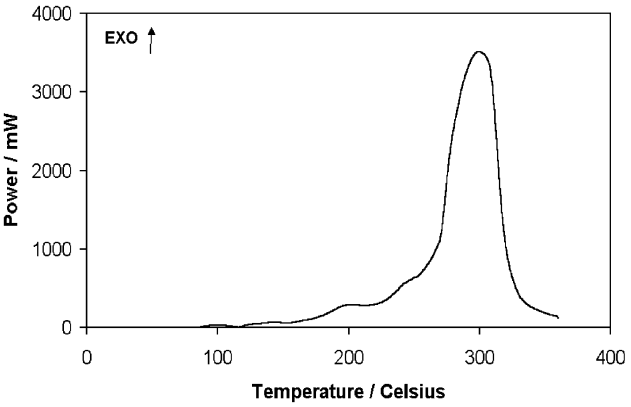

Fig. 4 DSC curve of uncalcined (as-prepared) mesoporous ceria-surfactant composite, displaying surfactant removal at about 573 K under an oxygen atmosphere.

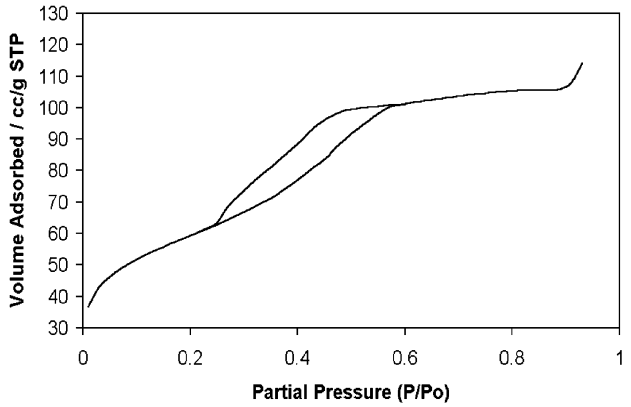

Fig. 3 BET adsorption and desorption isotherms for mesoporous ceria calcined at 673 K in air.

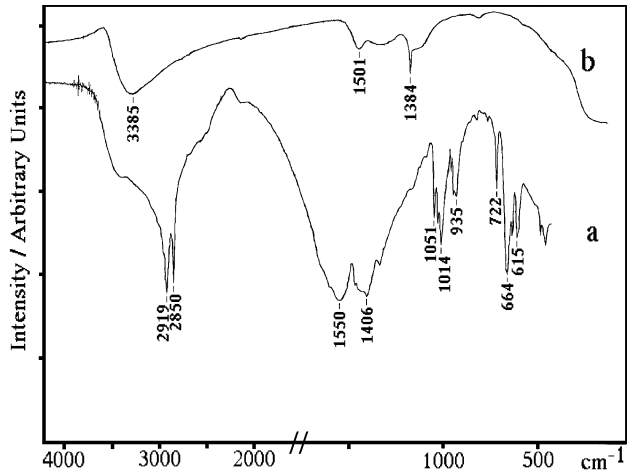

Fig. 5 Infrared spectra of (a) uncalcined ceria and (b) ceria calcined in air at 573 K.

traces recorded from tri-block templated inorganic mesoporous materials[9] and suggests that there is a single critical step in the template removal mechanism. This implies that mass-transport is not a rate-limiting step as diffusion control would be expected to result in much broader peaks. It is suggested therefore that the template oxidation process probably initiates using lattice oxygen available from the surface of the pore wall ceria (since the surface oxygen is extremely labile). This is the most likely source since the surfactant micelle arrangements packs the pores and atmospheric oxygen is hindered from entering the bulk of the material and the reaction would be heavily diffusionally controlled and broad DSC features would result. The very sharp nature of the exotherm observed here is thus completely consistent with a process which does not involve mass transport limitations implied by oxygen diffusion through the pore-template network. This mechanism involves the use of surface lattice oxygen in template removal and if this was the only reaction route possible would result in the eventual bulk reduction of the ceria and possibly result in pore collapse during exothermic re-oxidation of the ceria on exposure to ambient conditions. There is no evidence to support a very extensive involvement of the bulk lattice oxygen mediated template removal mechanism in the work reported here as described below.

The involvement of bulk fluorite (CeO_2) derived oxygen ions is not consistent with high angle PXRD profiles which show well-ordered stoichiometeric fluorite structures for all the materials prepared. This is thought to be related to the fact that the calcined materials were pre-dried at 423 K for 4 hours prior to calcinations (pre-dried meaning pre-calcination drying) to produce well-defined and crystalline pore walls. This preparative approach was based on the proposed reaction mechanism and observations of Knowles and Hudson who reported that controlled drying led to a greater degree of cross-linking within the hydrous oxide matrix resulting in densification and strengthening in addition to reduction of interfacial tension within the pores by removal of water.[15] In relation to the possible template removal model discussed above and first proposed by Trovarelli *et al.*[16] who suggested reduced ceria phases as a reaction product, studies of our calcined (T = 873 K) material by PXRD gave no evidence for the formation of reduced ceria phases and only ceria fluorite-type reflections were observed. Fig. 6(a) shows that well resolved fluorite reflections are observed even for the as-synthesised (uncalcined material). This is an unusual observation discussed further below. On calcination the only change in the fluorite features are associated with increased ordering or particle growth and consequent peak narrowing as seen in Fig. 6(b). Rietveld analysis provides no evidence for any gross non-stoichiometery (as indicated by unit cell site occupancy factors which are consistent with stoichiometeric CeO_2) and no new features or peak position shifts are apparent due to ordered CeO_{2-x} structures.[17] Whilst we cannot rule out the possibility of small non-stoichiometric regions in the ceria (as PXRD–Rietveld is not too sensitive to the small variations in oxygen content) it is clear that none of the well-known ordered reduced ceria phases are observed and essentially the PXRD details are not consistent with bulk reduction. The data presented here suggest a model that is essentially a combination of the two alternative reaction mechanisms presented by Trovarelli *et al.*[12] and Hudson and Knowles.[15] This model is as follows. During the drying (423 K) stage the acetate hydrous oxides crosslink extensively to form a densified oxide matrix around the template and this has considerable mechanical strength. Note that even at this stage the wall ceria has actually a quite distinct crystal structure (Fig. 6(a)) with some partial disorder. To our knowledge this is the first observation of crystalline ordered walls in mesoporous phases. This statement is discussed in detail below. Wall restructuring during template removal and higher temperature thermal treatment is accompanied by pore shrinkage in which the (100) reflection from the mesoporous array increased from 1.1° to 2° 2θ or a pore-to-pore dimension change of 70 Å to 40 Å and the high angle diffraction pattern becomes very highly ordered. Note that this is a very extensive decrease in pore-to-pore distance related to the degree of crystalline ordering obtained in the walls as described below. PXRD data below show that during template removal and calcination the pore wall thickness changes from about 6–10 nm consistent with the change in low angle peak position. It is proposed that oxidation of the template initially results from the reaction with surface lattice oxygen from the pore walls. As the reaction proceeds template is removed allowing rapid transfer of gas phase oxygen into the now partially void pore system and effective surface re-oxidation of ceria occurs. Note that even catalytic oxidation of methane begins on low surface area ceria at temperatures as low as 573 K[18] fully consistent with rapid surface oxygen mass transport at these temperatures. There is little tendency for complete pore collapse during the process of template removal because of the thermal stability of the crystalline ceria phase and if template removal is accompanied by reduction from a CeO_2 type species to CeO_{2-x} this process is accompanied by only relatively small amounts of bulk reaction (rather than surface reaction). It might be suggested that Trovarelli's observed pore collapse on template removal is related directly to shrinkage caused by having only non-dense non-crosslinked poorly defined pore walls and hydrous oxides as compared to the fluorite type phases seen in the walls in this work.

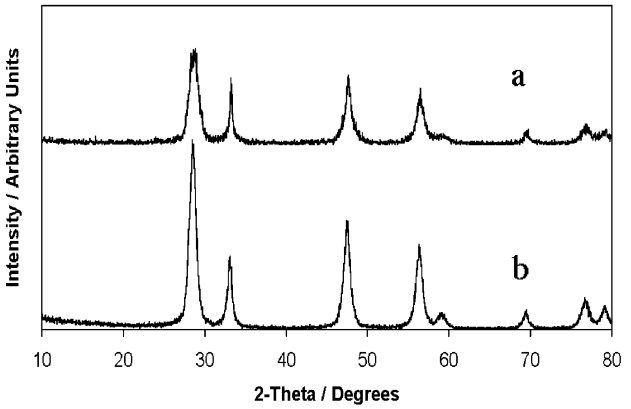

Fig. 6 PXRD diffractograms of the (a) as-synthesised ceria–surfactant composite and (b) the material after calcination at 873 K in air.

It is suggested that this is the first observation of crystalline pore walls in mesoporous systems. This claim must be explained in detail. Stucky *et al.* have reported crystallinity in many mesoporous systems prepared from tri-block poly-oxide systems.[9] However crystallinity must be carefully defined in this instance. In the work of these authors, as-calcined mesoporous TiO_2 showed some weak high angle X-ray diffraction features on a broad low angle background typical of amorphous materials.[9] It might be concluded that there is some crystalline material in the wall or some mesoporous titania has crystallised into a dense phase. Very sharp diffraction peaks are observed for as-synthesised chromium and copper systems however and Stucky *et al.* suggest these are lamellar systems and the crystalline phases are present in the layer structure[9] and may not relate to pore wall structure. However, good evidence for crystalline pore walls is presented for TiO_2, ZrO_2 and Nb_2O_5 structures.[9] On calcination of the organic–inorganic precursors to these materials, very broad high angle diffraction features are observed suggestive of a pore wall crystallite structure.[9] However, the crystallite sizes are of the order of 2 nm and the crystallinity, on the basis of PXRD and TEM data, is assigned to nanocrystallinity.[9] This is best thought of as the walls having a polycrystalline-type structure.

Quite clearly this is related to ordering of the walls over distances less than the wall thickness or pockets of local order in the general, very poorly ordered, wall structure.

The system described here is one of true crystallinity *i.e.* the crystallite size is of the order of the pore wall thickness and that the pore walls exhibit well-defined surface planes. This is clearly shown in the calcined material and even the as-prepared material where very high mesoporosity is demonstrated by very sharp intense low angle PXRD features (in stark contrast to the data of Stucky *et al.* where no high angle diffraction is observed prior to template removal[9]). Fig. 6 shows high angle diffraction patterns for the as-synthesised mesoporous ceria and after calcination at 873 K. It can be seen that both profiles have quite unusual variations in peak widths and do not show the expected decrease in peak with increasing angle. This is most obvious in Fig. 7 where the data for the as-synthesised material has been Rietveld fitted. The (111) reflection (about 29° 2θ) is relatively broad whilst the (200) reflection (about 33° 2θ) is very narrow. There are no signs of new features due to superstructures that may lead to splitting of *e.g.* the (111) reflection and resultant broadening due to poorly resolved overlapping features. All of the known fluorite distortions that might result in this type of effect have been trialed in Rietveld studies and none provided an adequate match to the experimental data. It can only be concluded that the material has quite unusual and distinctive particle shapes and the apparently very different half widths of the crystallographic reflections arise from directionalised effects, *i.e.* so that in certain crystallographic directions the sample appears to be thick and in other crystallographic directions the sample appears to be thin. This is not due to layering[19] (which would give highly asymmetric peaks) or preferred orientation[20] (very strong intensity effects) as close to 1 g quantities of fine powder material were analysed. Similar results have been obtained due to well-defined particle shapes exhibited by germanium nanowires.[21] As a consequence of the shape effects the Rietveld fit is very poor and clear peak width mismatch is illustrated in the residual plot at the lower part of Fig. 7. However the fit does indicate that the lattice spacing (a = 0.5410 nm) and the relative peak areas are fully consistent with stoichiometeric CeO_2. As well as the distortion of the (111) and (220) reflections all the other reflections show unusual peak shapes. This is illustrated in Fig. 8(a) which shows a peak fit to the data for the (220) reflection. The peak profile can only be adequately fitted by the presence of two features of differing widths when the residuals observed become very small. Scherrer analysis of the two features suggests particle sizes of 6.0 and 23.5 nm. The data are interpreted as follows. Broad peaks are observed for parts of the sample which are relatively thin *i.e.* for the reflections which define the surface planes of the walls; narrow reflections are observed for apparently thick parts of the sample *i.e.* for reflections from planes across the pore walls. This is illustrated in Fig. 8(b). It can be concluded that the pore wall is made up of (111) planes and thickness is of the order of 6 nm and this is fully consistent with the low angle PXRD data derived pore-to-pore distance of 7 nm obtained if relatively small pores are present (BJH pore size distribution data collected, shown in Fig. 9, suggest pore sizes of about 2.5 nm). Note also that the observation of (111) walls might have been expected as this is the only thermodynamically stable

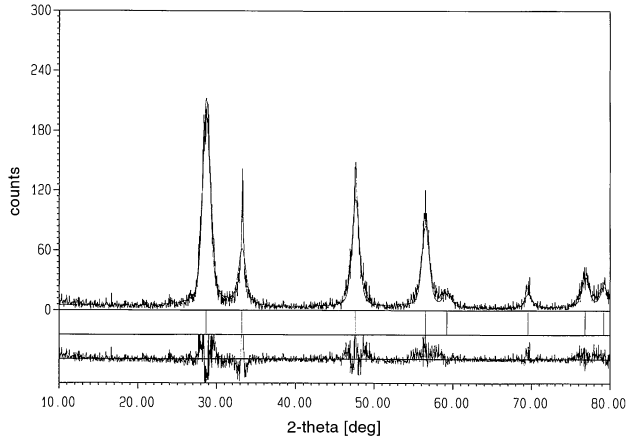

Fig. 7 PXRD diffractogram of as-prepared mesoporous ceria–surfactant composite and Rietveld fitted pattern. Shown below is the difference plot between experimentally collected data and the Rietveld generated match.

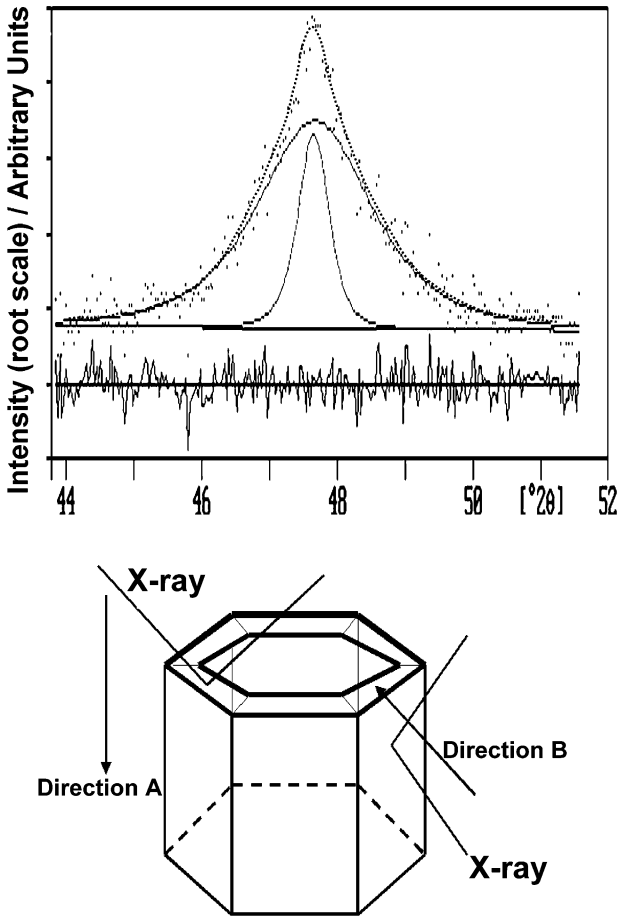

Fig. 8 (a) Deconvolution of the complex (220) ceria fluorite PXRD peak into two components. (b) Schematic figure showing how an ordered mesoporous crystalline material could simultaneously show narrow X-ray reflections from directions such as A (material has apparently large dimensions) and broad reflections from directions such as B (material has apparently small dimensions).

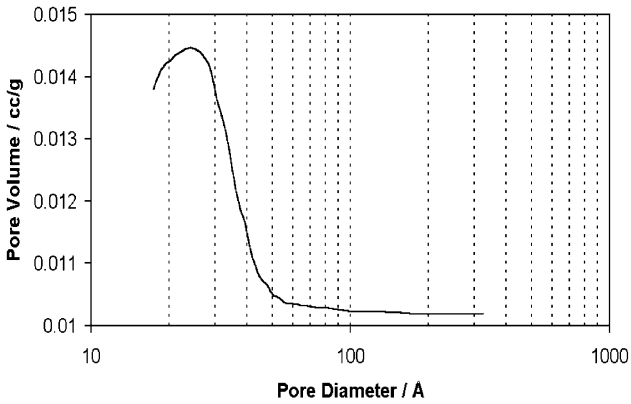

Fig. 9 BJH pore size distribution data collected for mesoporous ceria after calcination in air at 673 K.

surface plane of ceria.[22] The decrease in the pore–pore repeat distance noted on calcination is consistent with the preparation of much more ordered and consequently denser pore walls than previously observed. The claim that these mesoporous materials are amongst the very first of their kind to exhibit truly crystalline wall structures is clearly demonstrated by the data presented here.

Conclusion

In summary, careful control of reaction conditions and calcination regimes prevent complete pore collapse for an as-synthesised inorganic–organic mesoscopically ordered templated material and allow the formation of an ordered mesoporous ceria. The formation of stable mesoporous phases is related to low temperature removal of templating molecules and the use of cerium acetate to direct wall condensation. It is demonstrated that templating effects provide a synthetic means to create not just a high surface area form of ceria but to achieve a stable regular array of aligned pores in calcined materials. It is clearly demonstrated that the mesoporous materials obtained exhibit very well ordered crystalline pore walls. The development of new catalytic applications may result from this synthesis approach; certainly new cerias need to be prepared for use as catalysts in sooty diesel fuel exhaust systems.[23] This work is being extended to the preparation of doped ceria materials in an attempt to further stabilise and improve the quality of the mesoporous material and provide materials with high catalytic activity for high temperature oxidations.

Acknowledgements

The authors would like to gratefully acknowledge the assistance of Miriam Cotter and Mary Heapes for TEM training. Financial assistance is acknowledged from Enterprise Ireland under project BR/1997/198 for D. Lyons and the award of an Intel Ireland PhD Scholarship for K. Ryan. The advice of J.D. Holmes is also acknowledged.

References

1 A. Trovarelli, C. de Leitenburg, M. Boaro and G. Dolcetti, *Catal. Today*, 1999, **50**, 353.
2 *Non-Stoichiometric Oxides*, ed. O. T. Sorensen, Academic Press, New York, 1981.
3 A. Trovarelli, *Catal. Rev. Sci. Eng.*, 1996, **38**, 439.
4 H. C. Yao and Y. F. Y. Yao, *J. Catal.*, 1984, **89**, 254.
5 F. Fally, V. Perrichon, H. Vidal, J. Kaspar, G. Blanco, J. M. Pintado, S. Bernal, G. Colon, M. Daturi and J. C. Lavalley, *Catal. Today*, 2000, **59**, 373.
6 A. Martinez-Arias, M. Fernandez-Garcia, V. Ballesteros, L. N. Salamanca, J. C. Contesa, C. Otero and J. Soria, *Langmuir*, 1999, **15**, 4796.
7 C. T. Kresge, M. E. Leonowicz, W. J. Roth, J. C. Vartuli and J. S. Beck, *Nature*, 1992, **359**, 710.
8 A. Sayari, *Microporous Mater.*, 1997, **12**, 149.
9 D. Yang, D. Y. Zhao, D. I. Margolese, B. F. Chmelka and G. D. Stucky, *Nature*, 1998, **396**, 152; J. Y. Zheng, J. B. Pang, K. Y. Qiu and Y. Wei, *Microporous Mesoporous Mater.*, 2001, **49**, 189.
10 D. M. Lyons and M. A. Morris, Poster Presentation, Abstract only, *International Postgraduate Research Student Conference*, Dublin Institute of Technology, D. I. T., Dublin, 1998, p. 31.
11 P. T. Tanev, M. Chibwe and T. J. Pinnavaia, *Nature*, 1994, **368**, 321.
12 D. Terribile, A. Trovarelli, J. Llorca, C. de Leitenburg and G. Dolcetti, *J. Catal.*, 1998, **178**, 299.
13 D. Terribile, A. Trovarelli, C. de Leitenburg and G. Dolcetti, *Chem. Mater.*, 1997, **9**, 2676.
14 G. Meyer, *J. Alloys Compd.*, 2000, **300**, 113.
15 M. J. Hudson and J. A. Knowles, *J. Mater. Chem.*, 1996, **6**, 89.
16 D. Terribile, J. Llorca, M. Boaro, C. de Leitenburg, G. Dolcetti and A. Trovarelli, *Chem. Commun.*, 1998, 1897.
17 S. P. Ray and D. E. Cox, *J. Solid State Chem.*, 1975, **15**, 333.
18 M. O'Connell and M. A. Morris, *Catal. Today*, 2000, **59**, 387.
19 D. Yang, P. Westreich and R. F. Frindt, *Nanostruct. Mater.*, 1999, **12**, 467.
20 K. Tang, C. A. Wang, Y. Huang and X. Xu, *J. Alloys Compd.*, 2001, **329**, 136.
21 N. R. B. Coleman, K. M. Ryan, T. R. Spalding, J. D. Holmes and M. A. Morris, *Chem. Phys. Lett.*, 2001, **343**, 1.
22 J. Conesa, *Surf. Sci.*, 1995, **339**, 337.
23 J. Lemaire, D. Petta and O. Touret, Eur. Patent, 599717, 1994.